

**PIEZOELECTRIC ENHANCEMENT OF PVDF FILMS BY INDUCED
INTERNAL BUBBLE SHAPES**



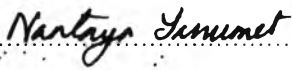
Ditthapun Suwansumpan

A Thesis Submitted in Partial Fulfilment of the Requirements
for the Degree of Master of Science
The Petroleum and Petrochemical College, Chulalongkorn University
in Academic Partnership with
The University of Michigan, The University of Oklahoma,
and Case Western Reserve University
2008

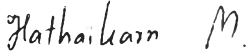
510303


Thesis Title: Piezoelectric Enhancement of PVDF Films by Induced Internal
Bubble Shapes
By: Ditthapun Suwansumpan
Program: Polymer Science
Thesis Advisors: Asst. Prof. Hathaikarn Manuspiya
Prof. Amar S. Bhalla

Accepted by the Petroleum and Petrochemical College, Chulalongkorn
University, in partial fulfilment of the requirements for the Degree of Master of
Science.

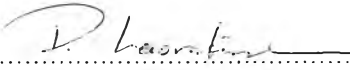

..... College Director
(Assoc. Prof. Nantaya Yanumet)

Thesis Committee:


.....
(Asst. Prof. Hathaikarn Manuspiya)


.....
(Prof. Amar S. Bhalla)


.....
(Assoc. Prof. Rathanawan Magaraphan)


.....
(Dr. Pitak Laoratanakul)

ABSTRACT

4972005063: Polymer Science Program

Ditthapun Suwansumpan: Piezoelectric Enhancement of PVDF Films by Induced Internal Bubble Shapes.

Thesis Advisors: Asst. Prof. Hathaikarn Manuspiya and Prof. Amar S. Bhalla 131 pp.

Keywords: Poly(vinylidene fluoride) / Microporous / Phase inversion / AZDC blowing agent / Dielectric properties / Piezoelectric coefficient

In this research, the effect of induced internal bubble shapes on dielectric behavior and piezoelectric properties in polyvinylidene fluoride (PVDF) was studied. The bubbles were created inside PVDF films by thermal phase inversion and AZDC blowing agent techniques. Subsequently, internal bubble shapes were observed using SEM and OM. The dielectric constant and the loss tangent of porous PVDF films were measured as a function of frequency range, 1 kHz-10 MHz, at room temperature by an impedance/gain-phase analyzer in different % porosities, sizes, structures, and shapes of bubbles. It was found that at high frequency the ellipsoid bubble shape showed more promising data, including a higher dielectric constant, less relaxation with frequency, and lower dielectric loss than spherical shaped. Also, the measured dielectric constant is fitted well with the Yamada model indicating 0-3 connectivity in PVDF/air bubble composites. Moreover, the ellipsoid shape can enhance the piezoelectric properties more than the spherical shape in PVDF films. Consequently, the PVDF with internal bubbles can be proposed as another candidate to use instead of ceramic-filled PVDF in lightweight piezoelectric applications.

บทคัดย่อ

คิตตพันธ์ สุวรรณสัมพันธ์ : การเพิ่มค่าสัมประสิทธิ์เพียโซอิเล็กตริกของฟิล์มโพลีไวนิลลิดีนฟลูออไรด์โดยศึกษาผลของรูปร่างฟองอากาศภายใน Piezoelectric Enhancement of PVDF Films by Induced Internal Bubble Shapes) อ. ที่ปรึกษา ผศ.ดร.หทัยกานต์ มนต์ปิยะ และ ศ.ดร.อมาร์ เอส บาลาร์ 131 หน้า

ในงานวิจัยนี้ ได้ศึกษารูปร่างของฟองอากาศที่มีผลต่อพฤติกรรมไดอิเล็กตริก เพียโซอิเล็กตริก และ เพียโซอิเล็กตริกของฟิล์มโพลีไวนิลลิดีนฟลูออไรด์(PVDF) ที่ถูกใส่ฟองอากาศเข้าไปข้างใน โดยใช้วิธี การกลับวัฏภาค (phase inversion) และ การเติมสารทำให้เกิดฟอง (blowing agent) ซึ่งโครงสร้างของคอมพอสิตจะถูกวิเคราะห์ด้วยกล้องจุลทรรศน์อิเล็กตรอนแบบส่องกราด (SEM) และกล้องจุลทรรศน์แบบแสง (OM) สำหรับค่าไดอิเล็กตริกและค่าการสูญเสียทางไดอิเล็กตริกของคอมพอสิตนี้จะถูกศึกษาในช่วงความถี่ (1 กิโลเฮิรต์-10 เมกกะเฮิรต์) ที่อุณหภูมิปกติ โดยมีอิทธิพลของ ปริมาณ, ขนาด, สัมฐานวิทยา และ รูปร่างของฟองอากาศที่แตกต่างกัน จากการทดสอบพบว่า ในช่วงความถี่ที่สูง ฟองอากาศในรูปแบบวงรี ให้ค่าไดอิเล็กตริกที่สูงขึ้น และให้ค่าการสูญเสียทางไดอิเล็กตริกที่น้อยกว่ารูปแบบวงกลม อีกทั้งฟองอากาศในรูปแบบวงรี ยังเพิ่มค่าสัมประสิทธิ์เพียโซอิเล็กตริกได้มากกว่ารูปแบบวงกลม นอกจากนี้แล้วยังได้พบว่า วัสดุคอมพอสิตระหว่างโพลีไวนิลลิดีนฟลูออไรด์และฟองอากาศนั้น เป็นการคอมพอสิตแบบ 0-3 โดยเทียบจากแบบสมการของยามาตะ ซึ่งวัสดุคอมพอสิตนี้ จะเป็นทางเลือกหนึ่งในการใช้งานทางเพียโซอิเล็กตริก ที่ต้องการน้ำหนักเบา ทนความร้อนและสารเคมีได้ดี

ACKNOWLEDGEMENTS

This thesis work is funded by the Petroleum and Petrochemical College, Polymer Processing and Polymer Nanomaterial Research Units, and the National Excellence Center for Petroleum, Petrochemicals, and Advanced Materials, Thailand.

First of all, I would like to express my profound gratitude to my advisors, Asst. Prof. Hathaikarn Manuspiya and Prof. Amar S. Bhalla for their invaluable support, encouragement, supervision, useful suggestions, valuable guidance, vital help and endless kindness throughout this research. Also, the author deeply thanks to all other committee members, Assoc. Prof. Rathanawan Magaraphan and Dr. Pitak Laoratanakul for taking time to serve on the committee and their valuable comments on thesis.

My special acknowledgement is expressed to Mr. Boonchana Mangkonkarn and Solvay Co, Ltd., for providing the PVDF materials to carry out this research. Gratitude is also extended to National Metal and Materials Technology Center (MTEC) for the electrical measurement and MTEC staffs for providing useful suggestion.

My sincere thanks go to all of the Petroleum and Petrochemical College's faculties who have tendered invaluable knowledge and go to the college staffs who give him invaluable assistance.

Memorable, the author would like to take this opportunity to thank all his PPC friends for their friendly assistance, cheerfulness, creative suggestions, and encouragement.

Last but not least, I warmly thank to all my family specially my father and my mother for their love, understanding and never lasting support during all these years. There are no words to express my gratitude to them and I love them for believing in me and never giving up on me.

TABLE OF CONTENTS

	PAGE
Title Page	i
Abstract (in English)	iii
Abstract (in Thai)	iv
Acknowledgements	v
Table of Contents	vi
List of Tables	ix
List of Figures	xi
 CHAPTER	
I INTRODUCTION	1
 II THEORETICAL BACKGROUND AND LITERATURE REVIEW	 3
 III EXPERIMENTAL	 25
 IV INTERNAL BUBBLE SHAPES EFFECT ON DIELECTRIC BEHAVIORS IN PVDF FILMS FROM PHASE INVERSION METHOD	 34
4.1 Abstract	34
4.2 Introduction	34
4.3 Experimental	35
4.4 Results and Discussion	37
4.5 Conclusions	62
4.6 Acknowledgements	63
4.7 References	63

CHAPTER		PAGE
V	EFFECT OF INTERNAL BUBBLE SHAPES ON DIELECTRIC BEHAVIORS IN POLY(VINYLDENE FLUORIDE) (PVDF) FILMS BY AZDC CHEMICAL BLOWING AGENT	66
	5.1 Abstract	66
	5.2 Introduction	66
	5.3 Experimental	67
	5.4 Results and Discussion	69
	5.5 Conclusions	83
	5.6 Acknowledgements	83
	5.7 References	84
VI	FERROELECTRIC AND PIEZOELECTRIC PROPERTIES OF 0-3 CONNECTIVITY AIR BUBBLES/PVDF COMPOSITES	86
	6.1 Abstract	86
	6.2 Introduction	86
	6.3 Experimental	87
	6.4 Results and Discussion	88
	6.5 Conclusions	93
	6.6 Acknowledgements	94
	6.7 References	94
VII	CONCLUSIONS AND RECOMMENDATIONS	96
	REFERENCES	97

APPENDICES	102
Appendix A Density of Porous films	102
Appendix B Porosity measurement of porous PVDF films	112
Appendix B Differential Scanning Calorimetry - DSC	116
Appendix D FT-IR of PVDF films	122
Appendix E Shape Parameter	129
CURRICULUM VITAE	130

LIST OF TABLES

TABLE		PAGE
CHAPTER II		
2.1	Comparison between the properties of PVDF and some common piezoelectric ceramic material	18
CHAPTER IV		
4.1	The Comparison between Density of Non-porous and Porous PVDF film	46
4.2	Average pore diameter of PVDF diluents systems with PVDF fraction 10 %wt	47
4.3	Average pore diameter of PVDF diluents systems with PVDF fraction 20 %wt	47
4.4	Average pore diameter of PVDF diluents systems with PVDF fraction 30 %wt	47
4.5	Porosity of porous PVDF films by different solvent (thickness 120 μm)	48
4.6	The variations of $F(\beta)$ % of solution-crystallized PVDF system	53
4.7	variations of $F(\beta)$ % of stretching PVDF films at solution-crystallized system	54
CHAPTER V		
5.1	The Comparison between Density of Non-porous and Porous PVDF film	73
5.2	Average pore diameter of PVDF with AZDC in different fraction (phr)	74

TABLE	PAGE
5.3 Porosity of porous PVDF films by different solvent (thickness 120 μm)	75

CHAPTER VI

6.1 Comparative data of d_{33} between non-stretching and stretching in PVDF films	90
6.2 The piezoelectric constant (d_{33}) of different porous structure in non-stretching PVDF films (spherical shape)	91
6.3 The piezoelectric constant (d_{33}) of different porous structure in stretching PVDF films (ellipsoidal shape)	92
6.4 The piezoelectric constant (d_{33}) of different bubble shapes in PVDF films	92

LIST OF FIGURES

FIGURE	PAGE
CHAPTER II	
2.1	The changes in a ferroelectric material that transforms from a para-electric cubic into ferroelectric tetragonal phase with temperature. 4
2.2	Ferroelectric $P-E$ hysteresis loop. Circles with arrows represent the polarization state of the material at the indicated fields. 5
2.3	The system of crystals in 32 classes. 6
2.4	The effect of piezoelectric material (a) direct piezoelectric effect (b) converse piezoelectric effect. 7
2.5	Specific direction and axis of piezoelectric. 8
2.6	Schematic diagram of the relation of the electromechanical coefficients for piezoelectric and pyroelectric materials. 8
2.7	The β form of PVDF. 10
2.8	Transitions from different conformations of PVDF to β -phase. 11
2.9	The interrelations among the four well-established phases of PVDF. 12
2.10	Dependence of relative amount of β -phase, $F(\beta)$, on (a) quenching temperatures and (b) Film thickness. 13
2.11	The effect of stretching rate (a) and ratio (b) in β / α ratio. 14
2.12	FTIR spectra of poled and non-poled samples of β -PVDF 500 cm^{-1} to 800 cm^{-1} region. 15
2.13	XRD pattern of tape cast PVDF sample with a poling field of (a) 300 MV/m and (b) 400 MV/m. 16
2.14	Loss of polarization potential in a homo PVDF polymer after annealing. 17

FIGURE	PAGE
2.15 Schematic sketch of a charged polypropylene foam electret, the charged voids form perfectly oriented macroscopic dipoles responsible for pyro- and piezoelectricity.	19
2.16 The structure of (a) Isotropic microporous membrane (b) Asymmetric membrane.	20
2.17 Concentration in casting solution on (a) average pore radius and (b) porosity of the resultant membrane.	21
2.18 SEM micrographs of two high porous (~75 vol %) PVDF homopolymer membranes in (a) a spongelike and (b) a finger-like texture.	22
2.19 The chemical structure of Azodicarbonamide.	24
CHAPTER III	
3.1 Fabrication procedure for PVDF films.	26
3.2 Fabrication procedure for micro-porous PVDF films.	27
3.3 Fabrication procedure for micro-porous PVDF films by blowing agent.	28
3.4 The schematic diagram of heater band.	29
3.5 Heat chamber system can classified into (a) temperature controller and heater band section.	30
CHAPTER IV	
4.1 The heater band equipment for stretching in PVDF films.	36
4.2 Photographs of porous PVDF films obtain from phase inversion technique by (a) DMAc (b) DMF, and (c) TEP.	37
4.3 SEM micrographs of porous PVDF film by operating T° at (a) 25, (b) 40, (c) 80, and (d) 120 $^{\circ}$ C.	38
4.4 Porous structure of PVDF films in coagulation bath at (a) 10, (b) 25 and (c) 50 $^{\circ}$ C, respectively.	39

FIGURE	PAGE
4.5 Comparison of PVDF microstructures formed in 3 different solvent (a) DMAc, (b) DMF, and (c) TEP.	40
4.6 SEM micrograph of cross-section of porous PVDF film cast from different polymer concentration (a) 10 (b) 20 and (c) 30 %wt by DMAc.	42
4.7 SEM micrograph of cross-section of porous PVDF film cast from different polymer concentration (a) 10 (b) 20 and (c) 30 %wt by DMF.	42
4.8 SEM micrograph of cross-section of porous PVDF film cast from different polymer concentration (a) 10 (b) 20 and (c) 30 %wt by TEP.	43
4.9 Micrographs of cross section of porous PVDF prepared with systems of different solvent.	44
4.10 The schematic drawing of spherical and ellipsoidal in porous PVDF films.	44
4.11 Structure of unstrained (spherical) and strained (ellipsoidal) of PVDF diluents systems with PVDF fraction of 20 wt% in (a),(b) DMAc, (c),(d) DMF, and (e),(f) TEP.	45
4.12 Compare porous PVDF films by (a) DMAc, (b) DMF, and (c) TEP.	46
4.13 Average pore sizes of porous PVDF films in different solvent and polymer concentration.	48
4.14 Relationship between PVDF concentration and % porosity.	49
4.15 TGA thermograms at 10 °C/min of nitrogen atmosphere of porous PVDF films in (a) different weight proportions (10, 20 and 30 %wt) (b) different solvent and different structure, (c) different bubble shapes.	50
4.16 DSC thermograms of porous PVDF Films which have (a) spherical and (b) ellipsoid shapes in different solvent system.	51

FIGURE	PAGE
4.17 FT-IR spectra of (a) Pure PVDF and porous PVDF with (b) DMAc, (c) DMF and (d) TEP solution-crystallized.	52
4.18 FT-IR spectra of stretching (a) flat PVDF and porous PVDF with (b) DMAc, (c) DMF and (d) TEP solution-crystallized.	53
4.19 XRD diffractograms of (a) non-stretching and (b) stretching porous PVDF films prepared by different solvents system: DMAc, DMF, and (d)TEP.	55
4.20 Comparing between (a) non-strained and (b) strained of non-porous PVDF films.	56
4.21 The frequency dependence of (a) the dielectric constant dielectric and (b) loss tangent of flat and porous PVDF films at different morphology structure.	56
4.22 The frequency dependence of the (a) dielectric constant and (b) dielectric loss tangent with frequency at room T ° of porous PVDF films by DMAc at in different % weight of polymer and different shape.	57
4.23 The frequency dependence of the (a) dielectric constant and (b) dielectric loss tangent with frequency at room T ° of porous PVDF films by DMF at in different % weight of polymer and different shape.	58
4.24 The frequency dependence of the (a) dielectric constant and (b) dielectric loss tangent with frequency at room T ° of porous PVDF films by TEP at in different % weight of polymer and different shape.	58
4.25 Frequency dependent (a),(c),(e) dielectric constant and (b),(d),(f) dielectric loss of porous PVDF films with different shape between spherical and ellipsoidal shape; (a),(b) from DMAC solvent, (c),(d) from DMF solvent and (e),(f) from TEP solvent.	60

FIGURE	PAGE
4.26 Plot of theoretical models and the measured dielectric constant for spherical shape at room temperature and 1 kHz.	61
4.27 Plot of theoretical models and the measured dielectric constant for ellipsoidal shape at room temperature and 1 kHz.	62

CHAPTER V

5.1 Assembly of thermal cabinet equipment for stretching PVDF films.	68
5.2 Porous PVDF films by AZDC compression molding technique.	69
5.3 PVDF Foam by (a) adding and (b) non-adding ZnO	70
5.4 Mixing between PVDF and AZDC by (a) internal and (b) external mixing.	70
5.5 The effect of chemical blowing agent on foam density of PVDF films from optical microscopy (a) 0.03%,(b) 0.3%, (c) 3% , (d) 0.01% (minimum) and (e) 7% (maximum) (phr).	71
5.6 The optical micrograph of spherical shape at (a) 0.03, (c) 0.3, (e) 3% and ellipsoidal shape at (b) 0.03, (d) 0.3, (f) 3% of AZDC in PVDF films.	72
5.7 The densities of porous PVDF in different AZDC concentrations (phr).	73
5.8 Average pore sizes of porous PVDF films in different AZDC fractions.	74
5.9 The effect of AZDC concentration (phr) on % porosity.	75
5.10 TGA thermograms of PVDF films in different (a) % BG and (b) shape of bubble.	76
5.11 DSC graphs of porous PVDF films in different (a) amount of air and (b) shapes.	77

FIGURE	PAGE
5.12 XRD diffractograms of porous PVDF films: (a) spherical and (b) ellipsoid shapes with different % AZDC or amount of air.	78
5.13 The frequency dependence of the (a) dielectric constant and (b) dielectric loss tangent with frequency at room T ° of porous PVDF films by compression molding at in different % weight of AZDC and different shape.	79
5.14 Frequency dependent (a) dielectric constant and (b) dielectric loss of porous PVDF films with different shape between spherical and ellipsoidal shape.	80
5.15 Comparing (a) dielectric properties and (b) dielectric loss of phase inversion and blowing agent techniques.	81
5.16 Plot of theoretical models and the measured dielectric constant of (a) spherical and (b) ellipsoidal shape in different air volume fractions at room temperature and 1 kHz.	82

CHAPTER VI

6.1 The SEM micrograph of porous PVDF by phase inversion with different shape of bubbles; (top) spherical and (bottom) ellipsoidal shape.	87
6.2 The OM micrograph of porous PVDF by AZDC compression molding with different shape of bubbles; (top) spherical and (bottom) ellipsoidal shape.	88
6.3 comparative hysteresis loops between non-strain and strain in non-porous PVDF films.	89
6.4 Comparative hysteresis loop between (a) spherical and (b) ellipsoidal bubble shapes in PVDF matrix by phase inversion method.	89

FIGURE	PAGE
6.5 Comparative hysteresis loop between (a) spherical and (b) ellipsoidal bubble shapes in PVDF matrix by phase inversion method.	90
6.6 Piezoelectric of flat PVDF films shown (a) non-stretching and (b) after stretching at 50 kV/mm.	91
6.7 Piezoelectric of spherical porous PVDF films shown (a) non-poling and (b) after poling in DMAc, DMF, and TEP at 50 kV/mm.	91
6.8 Piezoelectric of ellipsoidal porous PVDF films shown (a) non-poling and (b) after poling in DMAc, DMF, and TEP at 50 kV/mm.	92
6.9 Piezoelectric of porous PVDF films shown after poling (a) spherical and (b) ellipsoidal bubble shape at 50 kV/mm.	92